

Relaxation kinetics of biological dimer adsorption models

A. Vilfan

Cavendish Laboratory, Madingley Road, Cambridge CB3 0HE, UK

E. Frey

Abteilung Theorie, Hahn-Meitner-Institut, Glienickerstr. 100, D-14109 Berlin

F. Schwabl

Institut für Theoretische Physik, Technische Universität München, D-85747 Garching

(17/8/2001)

We discuss the relaxation kinetics of a one-dimensional dimer adsorption model as recently proposed for the binding of biological dimers like kinesin on microtubules. The non-equilibrium dynamics shows several regimes: irreversible adsorption on short time scales, an intermediate plateau followed by a power-law regime and finally exponential relaxation towards equilibrium. In all four regimes we give analytical solutions. The algebraic decay and the scaling behaviour can be explained by mapping onto a simple reaction-diffusion model. We show that there are several possibilities to define the autocorrelation function and that they all asymptotically show exponential decay, however with different time constants. Our findings remain valid if there is an attractive interaction between bound dimers.

Motor proteins are of fundamental importance for intracellular transport and many other biologically relevant transport processes. Recently, a large body of data on these proteins has been collected using a diverse set of experimental tools ranging from single-molecule mechanics [1] to biochemical methods [2]. In many instances these experimental systems are both versatile experimental techniques and interesting non-equilibrium model systems. One system of particular interest is a standard method from biophysical chemistry known as “decoration experiments” [2]. Here monomeric or dimeric motor enzymes are deposited on their corresponding molecular tracks at high densities (see fig. 1a). For kinesin motors, these tracks are microtubules, hollow cylinders usually consisting of 13 protofilaments. The kinesin binding sites are located on the β subunits which form a helical (wound-up rhombic) lattice with a longitudinal periodicity of 8 nm. Decoration techniques have traditionally been used to investigate the structure and the binding properties of kinesin [2] *i.e.* after waiting for the system to equilibrate the binding stoichiometry is determined and the structure by cryo-electron microscopy followed by 3D image reconstruction.

These experiments call for a theoretical analysis of dimer adsorption kinetics with competing single and double bound dimers and a finite detachment rate. For a quantitative analysis of decoration data [3] one needs to know the binding stoichiometry in the equilibrium state in terms of binding constants for the first and second head of the dimer molecule. The dynamics of the approach to equilibrium is useful to estimate when an experimental system can be considered as equilibrated [4]. Even more importantly, time-resolved decoration experiments (e.g. by using motor enzymes labelled by some fluorescent marker) combined with our theoretical analysis could provide new information about reaction rates which are to date not known completely. Understanding the kinetics of passive motors is undoubtedly a necessary prerequisite for studying the more complicated case of active motors at high densities. The model is also interesting in its own right since it contains – as detailed below – some novel features of non-equilibrium dynamics of dimer models which have not been discussed previously.

There seems to be convincing evidence that kinesin heads can bind on two adjacent binding sites only in longitudinal but not in lateral direction [2]. This introduces a strong uniaxial anisotropy and distinguishes the adsorption process of protein dimers from simple inorganic dimers. If we take into account only steric interactions and (for now) neglect nearest neighbour attractive interaction, we are left with a one-dimensional problem of kinesin dimers decorating a single protofilament (one-dimensional lattice). Then our model is defined as follows. Kinesin is considered as a dimeric structure with its two heads tethered together by some flexible joint. Hence each dimer (kinesin protein) can bind one of its two heads (motor domains) to an empty lattice site [3]. The binding rate $k_{+1}c$ for this process is proportional to the solution concentration c of the dimeric proteins. Successively, the dimer may either dissociate from the protofilament with a rate k_{-1} or also bind its second head to an unoccupied site in front (f) of or behind (b) the already bound head. Since kinesin heads and microtubules are both asymmetric structures the corresponding binding rates k_{+2}^f and k_{+2}^b are in general different from each other. The reverse process of detaching a front or rear head occurs at rates k_{-2}^f and k_{-2}^b . A reaction scheme with all possible processes and their corresponding rate constants is shown in fig. 1b.

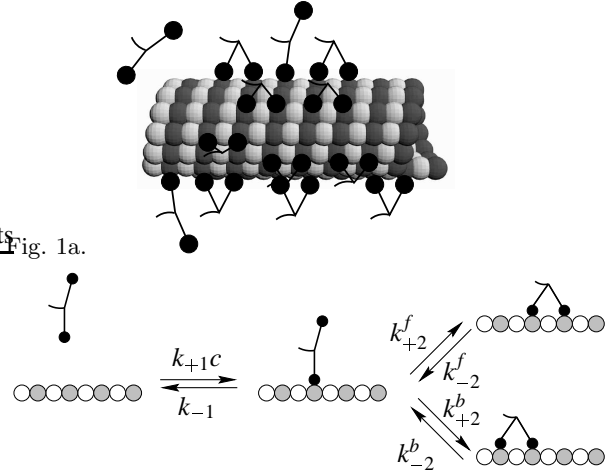


Fig. 1a.

Fig. 1b.

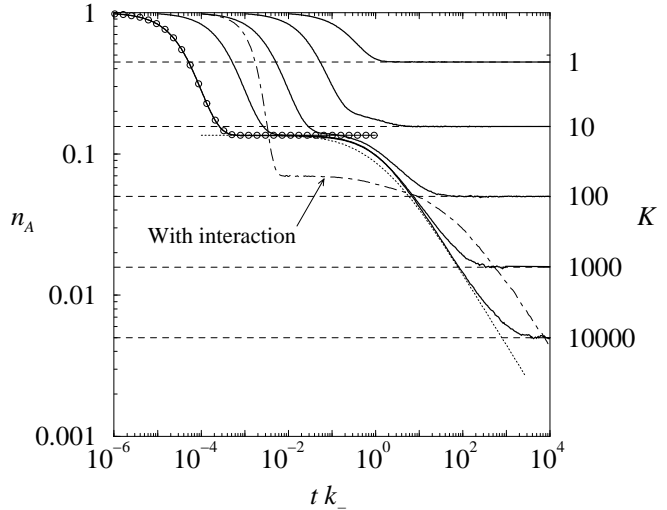


Fig. 2.

FIG. 1. a) Kinesin dimers can bind one head or both heads to a one-dimensional lattice (tubulin protofilament). Binding sites are located on β -tubulin subunits (dark) while α -subunits (bright) are irrelevant for our study. b) Reaction scheme for all binding and unbinding processes.

FIG. 2. Vacancy concentration as a function of time t for $K = k_+c/k_- = 1, \dots, 10000$. Dashed lines show the steady state concentration $n_0 = 1/\sqrt{1+4K}$ at given K . The line with circles shows the short-time limit for $K = 10000$ [5], and the dashed line the result of the reaction-diffusion model (Eq. 2). The thin dot-dashed curve shows the behaviour for $K = 100$ with an attractive interaction between bound dimers with parameters $A = 10$ and $B = 1/10$ (a dimer is 10 times as likely to associate to and 10 times less likely to dissociate from a certain site if one of the neighbours is present).

Since there is no energy source in the system (unlike situations where ATP is being hydrolysed), the reaction rates obey the principle of detailed balance. As a consequence, the reaction rates are actually not independent from each other but the ratio of the on- and off-rates has to equal the equilibrium binding constant $K_2 = k_{+2}^b/k_{-2}^b = k_{+2}^f/k_{-2}^f$; similarly we have $K_1 = k_{+1}/k_{-1}$. A particular coverage of the lattice is described as a sequence of dimers bound with both heads (D), one head only (1) and empty sites (0). We denote the probabilities to find a certain lattice site in one of these states by $2n_D$, n_1 and n_0 , respectively. Of course, normalisation of the probabilities requires $n_0 + n_1 + 2n_D = 1$.

We start our analysis with the stoichiometry of the final steady state. Important information can be gained already by exploiting the symmetries of the kinetic process. The reaction scheme in fig. 1b (including steric constraints) remains invariant under the following transformation: (I) all dimers bound on a single head are replaced by vacant sites and vice versa ($0 \leftrightarrow 1$), while dimers bound with both heads are kept as they are ($D \leftrightarrow D$). (II) The attachment and detachment rate of the first head are exchanged and the forward/backward binding rates of the second head are mirrored ($k_{+1}c, k_{+2}^f \leftrightarrow (k_{-1}, k_{+2}^b)$). Since the coverage in the steady state is only a function of K_1c and K_2 (see below) this symmetry implies that the mean number of dimers attached with both heads $n_D(K_1c, K_2)$ is invariant against interchanging the attachment and detachment rates of the first head, $n_D(1/(K_1c), K_2) = n_D(K_1c, K_2)$. Similarly, the mean total number of bound heads per lattice site (often simply called binding stoichiometry), $\nu = 2(n_1 + n_D)$, obeys the symmetry relation $\nu(1/(K_1c), K_2) = 2 - \nu(K_1c, K_2)$. Thus we conclude that n_D reaches its maximum at $K_1c = 1$ where $\nu = 1$.

We determine the actual value of the mean occupation numbers in the steady state using detailed balance and the fact that the dimers have only a hard-core interaction. Hence the probability to find a certain sequence of 0 's, 1 's and D 's (e.g. "0,1,D,D,1,D") has to be invariant against permutations of these states. In such a random sequence the probabilities to find a particular state 0 , 1 or D at a certain place are given by $p_i = n_i/(n_0 + n_1 + n_D)$. Detailed balance requires that for each pair of possible configurations, their probabilities are in the same ratio as the transition rates between them. Hence the ratio of probabilities to find a sequence with a 1 or 0 at a certain place is $p_1/p_0 = k_{+1}c/k_{-1} = K_1c$. Similarly, we get for transitions between D and 01 : $p_D/p_0p_1 = k_{+2}^{b,f}/k_{-2}^{b,f} = K_2$. These two equations, together with the normalisation condition, uniquely determine the values n_0 , n_1 and n_D . The stoichiometry, i.e. the total number of heads per binding site $\nu = 2(n_1 + n_D)$ is given by

$$\nu = 1 + \frac{K_1 c - 1}{K_1 c + 1} \left(\frac{4K_1 K_2 c}{(1 + K_1 c)^2} + 1 \right)^{-\frac{1}{2}}. \quad (1)$$

The number of dimers bound with both heads per lattice site reaches its maximum $n_D^{\max} = (1 - 1/\sqrt{K_2 + 1})/2$ for $K_1 c = 1$.

We now turn to the dynamics of the biological dimer model. In order to avoid unnecessary complications we restrict ourselves to the limit $K_2 \rightarrow \infty$ with $K = K_1 K_2 c$ fixed. Then our model reduces to a dimer deposition-evaporation model where the dimers can only bind and unbind with both heads at the same time. The vacancy concentration in the steady state then simplifies to $n_0 = 1/\sqrt{1 + 4K}$. This simplified model still captures all the essential aspects of the non-equilibrium dynamics. Similar dimer adsorption models have been studied previously [6–8]. Privman and Nielaba [6] studied the effect of diffusion on the dimer deposition process. There are several key differences to our model, the most important of which is that diffusion without detachment results in a 100% saturation coverage, whereas a model with detachment leads to a limiting coverage whose value depends on the binding constants of the first and second head (see eq. 1). This also has important implication on the dynamics as discussed below. For example, as a consequence of a finite coverage the final approach to equilibrium is not a power law but exponential and there are, in addition, interesting temporal correlations in the fluctuations in the steady state. Stinchcombe and coworkers [7,8] studied the effect of detachment on the adsorption kinetics but allowed for regrouping of attached dimer molecules (two monomers that belonged to different dimers during attachment can form a dimer and detach together). While such processes are allowed for some types of inorganic dimers, they are certainly forbidden for dimer proteins like kinesin where the linkage between its two heads is virtually unbreakable. If regrouping is allowed the *steady state* auto-correlation functions for the dimer density shows an interesting power-law decay $\propto t^{-1/2}$ [7,8]. If it is forbidden this power-law decay is lost (and becomes an exponential to leading order) due to the permanent linkage between the two heads of the dimer. Intuitively this may be understood as follows: only if regrouping of dimers is allowed are there locally jammed configurations (Néel-like states, “101010”, with alternating occupied and unoccupied sites in which neither attachment nor detachment of dimers is possible) in the final steady state which slow down the dynamics. In addition, we will show that the autocorrelation functions of the dimer and the vacancy occupation number show strong differences in shape and typical times scales of relaxation.

The basic kinetic steps in the reduced model are deposition without overlap and evaporation without regrouping of the dimers; the effective attachment and detachment rates k_{\pm} in terms of the original model are $k_{\pm} = k_{1\pm}(k_{\pm}^f + k_{\pm}^b)/(k_{-1} + k_{+2}^f + k_{+2}^b)$. Processes in which one head detaches on one side and subsequently attaches on the other side also lead to *explicit* diffusion with a rate $r_d = k_{+2}^f k_{+2}^b / (K_2(k_{-1} + k_{+2}^f + k_{+2}^b))$. This feature is not essential since it can be incorporated in the effective diffusion introduced later. It will hence be disregarded in what follows (if one of the rates $k_{+2}^{f,b}$ is small, it is negligible anyway). Note that as a consequence of detailed balance the diffusion of dimers is symmetric despite the asymmetry in reaction rates.

To study the kinetics we choose the initial condition as typically used in an experiment, namely an empty lattice. Figure 2 shows simulation data [9] for the average vacancy concentration as a function of time for a set of binding constants $K = k_+ c / k_- \equiv K_1 K_2 c$. We find qualitatively very different approaches to the final steady state depending on the value of the constant K . For $K \ll 1$, where the off-rate k_- is much larger than the on-rate $k_+ c$, there is no crowding on the lattice and the dimeric nature of the molecules does not affect the approach to equilibrium, which is, like for monomers, exponential with a decay rate k_- . In the opposite limit, $K \gg 1$, we find a *two-stage relaxation* towards the steady state. The vacancy concentration as a function of time reveals *four regimes*, an initial attachment phase, followed by an intermediate plateau, then a power-law decay and finally an exponential approach towards equilibrium. At short time scales, $t \ll k_-^{-1}$, when only deposition processes are frequent but detachment processes are still very unlikely, the kinetics of the model is equivalent to Flory’s random sequential dimer adsorption model [10,11]. There is an initial decay obeying the kinetics described in [5,12] with a vacancy concentration $n_0(t) = \exp(-2 + 2e^{-k_+ c t})$. The vacancy concentration locks at an intermediate plateau $n_0 = e^{-2}$ [10] in the time interval between the characteristic attachment time $\tau_+ = 1/(k_+ c)$ and detachment time $\tau_- = 1/k_-$. This Flory plateau represents a configuration in which all remaining vacancies are isolated, causing the system to be unable to accommodate for the deposition of additional dimers. The secondary relaxation process towards the final steady state is enormously slowed down. It shows a broad time domain with a power-law $\propto t^{-1/2}$ instead of a simple exponential decay. Similar multi-stage relaxation processes have been observed in dimer models with diffusion but no detachment [6], the key difference being that the detachment process implies that the steady state has a finite vacancy density and the final approach to the steady state remains not a power law but becomes exponential. There are also interesting similarities. In particular, in both models a large portion of the final approach to the steady state is mediated by the annihilation of vacancies. This behaviour can be explained by introducing a particle representation in the following way (analog to the adsorption-diffusion model [6]). We denote each vacancy on the lattice as a “particle” A , and each bound dimer as an inert state (00) .

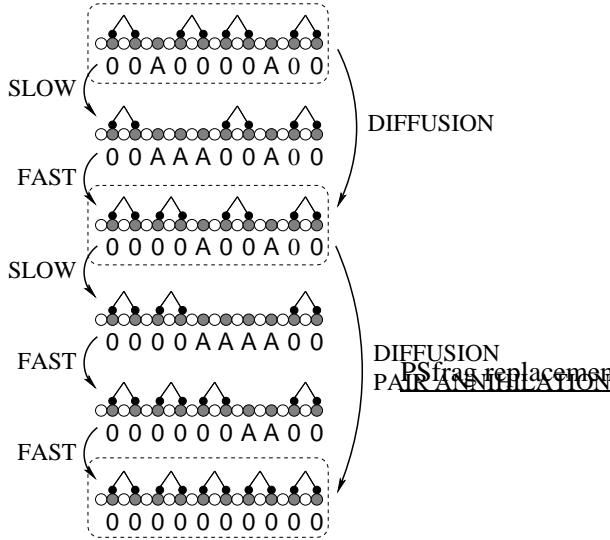


Fig. 3.

FIG. 3. Time evolution of a state, consisting of attachment (fast) and detachment (slow) events. The coarse-grained interpretation includes only long-living states (in boxes). The effective steps include diffusion, pair annihilation and pair creation (not shown).

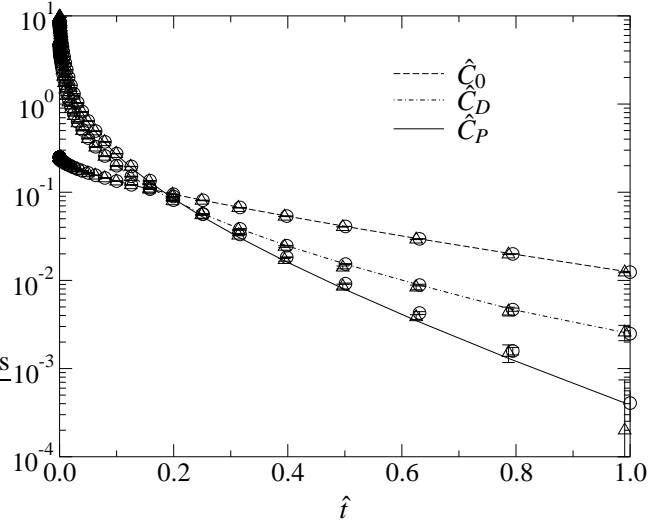


Fig. 4.

FIG. 4. Scaled equilibrium autocorrelation functions for $\hat{C}_0(\hat{t}) = KC_0(t)$, $\hat{C}_D(\hat{t}) = C_D(t)$ and $\hat{C}_P(\hat{t}) = KC_P(t)$, $\hat{t} = k_-t/K$. The function $\hat{C}_P(\hat{t})$ is compared with the analytical calculation from ref. [13] (solid line). Simulation data were obtained with $K = 100$ (circles, for C_0 and C_D connected with dot-dashed and dashed lines) and $K = 400$ (triangles).

The detachment of a dimer then corresponds to a pair creation process $00 \rightarrow AA$, and the decoration process to pair annihilation $AA \rightarrow 00$. Since we consider the limit $K \gg 1$, states with two vacancies A on neighbouring sites have a very short lifetime. We may thus introduce a coarse-grained model by eliminating these states (see fig. 3). Then processes like $A00 \rightarrow AAA \rightarrow 00A$ result in an *effective diffusion* for particle A with a hopping rate $r_{\text{hop}} = k_-/2$ and an effective step width of two lattice sites. *Pair annihilation*, $AA \rightarrow 00$, occurs with a rate k_+c . *Pair creation*, on the other hand, occurs mainly through the process $0000 \rightarrow 00AA \rightarrow AAAA \rightarrow A00A$; the corresponding rate is $k_-/3K$ per lattice site and hence largely suppressed with respect to the annihilation process as long as the particle concentration is far above its steady-state value. Other processes involve more particles and are of higher order in terms of a power series in K^{-1} . They are negligible for $n_A \ll 1$ and $K \gg 1$. In summary, for $K \gg 1$, our dimer model can be mapped onto a one-particle reaction-diffusion model $A + A \rightarrow 0$. Pair creation processes, $0 \rightarrow A + A$, are highly suppressed and do not play any role until the system comes close the steady state.

Models like the simple reaction-diffusion model $A + A \rightarrow 0$ show interesting non-equilibrium dynamics [14–16]. One can show [17,18] that asymptotically the particle density $n_A(t)$ decays algebraically, $n_A(t) \propto t^{-1/2}$ which nicely explains the slow decay observed in simulation data (see fig. 2). Note that a mean-field like rate equation approach would predict $n_A(t) \propto t^{-1}$. In our analysis we can even go beyond the asymptotic scaling analysis and try to compare with exact solutions of the model for a random initial distribution with density p by Krebs *et al.* [19]. They find (adapted to our situation with two-site hopping)

$$n_A(t) = \frac{1}{2\pi} \int_0^2 du \frac{\sqrt{u(2-u)} p^2 e^{-16ur_{\text{hop}}t}}{u(u(\frac{1}{2}-p) + p^2)}. \quad (2)$$

Its asymptotic limit (first determined by Torney and McConnell [17]) reads $n_A = (32\pi r_{\text{hop}}t)^{-1/2}$; note that it is independent of the initial particle concentration in the Flory plateau p .

Our Monte-Carlo data (see fig. 2) are in excellent agreement with the predictions of eq. 2. Minor deviations at times between the plateau and the power-law decay are due to the assumption of a random particle distribution underlying the derivation of eq. 2; the random sequential adsorption process leads to some particle correlations in the intermediate plateau regime [12], but they do not affect the asymptotic behaviour as they are only short-ranged. The results from the $A + A \rightarrow 0$ model also become invalid for very long times where the particle concentration comes close to its equilibrium value. In this limit the dynamics becomes scale-invariant [20]. The particle concentration can

be written in scaling form $n_A(t) = K^{-1/2} \hat{n}(r_{\text{hop}} t / K)$ with a diverging characteristic time scale $\tau_K \propto K$.

A limitation of the above mapping becomes evident if one considers the equilibrium autocorrelation functions. Contrary to conventional models there are three different autocorrelation functions with different functional forms (fig. 4). $C_0(t) = \langle \hat{n}_{0_i}(t_0) \hat{n}_{0_i}(t_0 + t) \rangle - \langle \hat{n}_{0_i} \rangle^2$ describes the correlation function of the probability to find a vacancy at a certain lattice site. C_D is the equivalent quantity defined from the probability to find a dimer on a certain pair of sites $\hat{n}_{D_{i,i+1}}$ and C_P from the probability to find a vacancy on at least one from a pair of neighbouring sites, $\hat{n}_{0_i} + \hat{n}_{0_{i+1}} - \hat{n}_{0_i} \hat{n}_{0_{i+1}}$. For $K \gg 1$ the autocorrelation functions become scale invariant as well. Their scaling form reads $\hat{C}_0(\hat{t}) = K C_0(t)$, $\hat{C}_D(\hat{t}) = C_D(t)$ and $\hat{C}_P(\hat{t}) = K C_P(t)$ with $\hat{t} = k_- t / K$. The latter corresponds to the autocorrelation function in a reaction-diffusion model $A + A \leftrightarrow 0$, which has recently been calculated analytically in ref. [13]

$$\hat{C}_P(\hat{t}) = \left(\frac{e^{-2\hat{t}}}{\sqrt{2\pi\hat{t}}} - \text{Erfc} \sqrt{2\hat{t}} \right) \text{Erfc} \sqrt{2\hat{t}}, \quad \text{with} \quad \text{Erfc}(x) = \frac{2}{\sqrt{\pi}} \int_x^\infty e^{-y^2} dy. \quad (3)$$

The other two functions decay on the same time-scale, but with different prefactors. The reason is that even if a pair of vacancies annihilates, the system still keeps memory on whether the surrounding dimers were located on even or odd locations and this gives those correlation functions that distinguish between even and sites a longer decay time.

Finally, we would like to note that an attractive interaction between attached dimers plays an important role in some cases. In the case of kinesin, there has been an observation of coexisting empty and decorated domains which can only be explained by an attractive interaction [3]. Similar observation has been done on actin decorated with myosin [21] and tropomyosin [22]. We introduce the interaction by assuming that a dimer is more likely to bind to a pair sites if one or two neighbours are already bound. The binding rate then becomes Ak_+ (one neighbour bound) or A^2k_+ (both neighbours bound). Similar, we assume that a dimer with one bound neighbour dissociates with rate Bk_- and that a dimer with two bound neighbours dissociates with rate B^2k_- . This interaction changes both relaxation stages quantitatively. First, the vacancy concentration on the intermediate plateau lowers since the interaction improves the formation of contiguous clusters during the first stage. Second, the diffusional relaxation slows down since the detachment rate decreases. And finally, the equilibrium vacancy concentration decreases. Nevertheless, interacting models show the same two-stage relaxation behaviour. An example of a model with interaction is shown by the dot-dashed line in fig. 2. We therefore expect that many qualitative conclusions from this article will apply to a much wider range of biological adsorption problems such as the binding of double-headed myosin [21] or tropomyosin [22].

We would like to thank E. Mandelkow and A. Hoenger for helpful discussion about microtubule decoration experiments and their relevance for studying motor proteins. We have also benefited from discussions with T. Franosch, J. Santos, G. Schütz and U.C. Täuber. Our work has been supported by the DFG under contract nos. SFB 413 and FR 850/4-1. E.F. acknowledges support by a Heisenberg fellowship from the DFG under Grant no. FR 850/3-1.

- [1] MEHTA A. D. *et al.*, *Science*, **283** (1999) 1689.
- [2] MANDELKOW E. and HOENGER A., *Curr. Opin. in Cell Biol.*, **11** (1999) 34, for latest results see HOENGER A. *et al.*, *J. Molec. Biol.*, **297** (2000) 1087.
- [3] VILFAN A. *et al.*, *J. Molec. Biol.* (2001) in press.
- [4] With reaction rates from [23] ($k_- \approx 0.001 \text{ s}^{-1}$ with AMP-PNP or without nucleotide) and assuming that there is no explicit diffusion ($r_d \ll k_-$) the relaxation time for a high kinesin concentration ($K = 100$) can be as long as 10^5 s . On the other hand, in the presence of ADP ($k_- \approx 1 \text{ s}^{-1}$) and $K = 10$ the relaxation time can be as short as 10 s . Some care has to be taken as these results were obtained with kinesin attached to beads.
- [5] MCQUISTAN R. B. and LICHTMAN D., *J. Math. Phys.*, **9** (1968) 1680.
- [6] PRIVMAN V. and NIELABA P., *Europhys. Lett.*, **18** (1992) 673.
- [7] BARMA M., GRYNBERG M. D. and STINCHCOMBE R. B., *Phys. Rev. Lett.*, **70** (1993) 1033.
- [8] STINCHCOMBE R. B., GRYNBERG M. D. and BARMA M., *Phys. Rev. E*, **47** (1993) 4019.
- [9] For a Java applet of the simulation see <http://www.ph.tum.de/~avilfan/relax>.
- [10] FLORY P. J., *J. Am. Chem. Soc.*, **61** (1939) 1518.
- [11] The case without explicit diffusion corresponds to the “standard” [10] dimer filling model and the diffusive case to the “head-on” dimer filling model [24,25] with the final vacancy concentration 0.1233. The final configuration is independent of the asymmetry in the binding rates.
- [12] EVANS J. W., *Rev. Mod. Phys.*, **65** (1993) 1281.

- [13] BARES P.-A. and MOBILIA M., *Phys. Rev. E*, **59** (1999) 1996. Note that the described solution is derived for a parameter set which requires a fine tuning between diffusion, pair-creation and annihilation rate. In our model this relation is not fulfilled. But, this difference becomes irrelevant in the scaling limit, since their and our model can be mapped onto each other by introducing a short-ranged interaction between particles. See also PARK S.-C., PARK J.-M. and KIM D., *Phys. Rev. E*, **63** (2001) 057102 for a comment about the validity of the analytical approximation. The observed deviations however do not affect the scaling limit.
- [14] V. PRIVMAN, editor, *Nonequilibrium statistical mechanics in one dimension*, Cambridge University Press, Cambridge, 1997.
- [15] MATTIS D. C. and GLASSER M. L., *Rev. Mod. Phys.*, **70** (1998) 979.
- [16] SCHÜTZ G., Reaction-diffusion mechanisms and quantum spin systems, in *Field theoretical tools for polymer and particle physics*, edited by H. MEYER-ORTMANN and A. KLÜMPER, volume 508 of *Lecture Notes in Physics*, Springer, Berlin, 1998.
- [17] TORNEY D. C. and MCCONNELL H. M., *J. Phys. Chem.*, **87** (1983) 1941.
- [18] TOUSSAINT D. and WILCZEK F., *J. Chem. Phys.*, **78** (1983) 2642.
- [19] KREBS K., PFANMÜLLER M. P., WEHEFRITZ B. and HINRICHSSEN H., *J. Stat. Phys.*, **78** (1995) 1429.
- [20] RÁCZ Z., *Phys. Rev. Lett.*, **55** (1985) 1707.
- [21] ORLOVA A. and ENGELMAN E., *J. Molec. Biol.*, **265** (1997) 469.
- [22] WEGNER A., *J. Molec. Biol.*, **131** (1979) 839.
- [23] HANCOCK W. and HOWARD J., *Proc. Natl. Acad. Sci. (USA)*, **96** (1999) 13147.
- [24] PAGE E. S., *J. Roy. Statist. Soc. B*, **21** (1959) 364.
- [25] NORD R. S. and EVANS J. W., *J. Chem. Phys.*, **93** (1990) 8397.